

Weak Localization in Chaotic versus Nonchaotic Cavities: A Striking Difference in the Line Shape

A. M. Chang, H. U. Baranger, L. N. Pfeiffer, and K. W. West

AT&T Bell Laboratories, 600 Mountain Avenue, Murray Hill, New Jersey 07974-0636

(Received 26 May 1994)

We report experimental evidence that chaotic and nonchaotic scattering through ballistic cavities display distinct signatures in quantum transport. In the case of nonchaotic cavities, we observe a linear decrease in the average resistance with magnetic field which contrasts markedly with a Lorentzian behavior for a chaotic cavity. This difference in line shape of the weak-localization peak is related to the differing distribution of areas enclosed by electron trajectories. In addition, periodic oscillations are observed which are probably associated with the Aharonov-Bohm effect through a periodic orbit within the cavities.

PACS numbers: 72.20.My, 05.45.+b, 72.15.Gd, 73.40.Kp

A central question for “quantum chaos” in open systems is whether scattering from a system which classically exhibits chaotic dynamics will give rise to observable quantum signatures distinct from a nonchaotic system [1]. Considerable attention has been focused on the connection between the quantum S matrix and the classical dynamics [1–8]. Recent theoretical studies indicate that the quantum transmission probability, which is intimately related to the conductance of a microstructure, directly reflects the classical behavior [3,5,7,8]. In particular, in the chaotic case the statistical distribution of the quantum transmission probability as a function of either the incident momentum k [2] or magnetic field B [3] reflects the existence of a single classical trapping time scale; the power spectrum of the conductance fluctuations $G(k)$ or $G(B)$ decays via a single exponential for several decades. In addition, the average transport should show a negative magnetoresistance peak, known as weak localization (WL), centered about $B = 0$ with a line shape in the form of a Lorentzian [7]. In direct contrast, in the nonchaotic (integrable) case, the lack of a single time scale gives rise to a power law tail in the power spectrum for large frequencies [5–8] and a highly unusual linear line shape for the weak-localization peak [7].

In this Letter, we focus on the WL line shape. We present experimental evidence that the shape is strikingly different for transport through a ballistic chaotic cavity in the form of a stadium versus a nonchaotic cavity in the form of a circle. Specifically, we observe a Lorentzian line shape for the stadium and a linear line shape for the circle down to $\sim 0.09B_{1/2}$, where $B_{1/2}$ refers to the half width at half maximum. Our results are obtained in microstructures fabricated from a very high quality GaAs/Al_xGa_{1-x}As heterostructure crystal. For each type of cavity, 48 devices are measured at once to average out the universal conductance fluctuations. We directly compare these results with numerical calculations of nominally identical cavities; the good agreement between theory and experiment strongly supports our view that the

difference in line shape is caused by the difference in the character of the classical dynamics.

We extend our basic observation in two different ways. (1) As the temperature is lowered from 4.2 K to 50 mK, the WL in the stadium remains Lorentzian while that in the circle evolves from a Lorentzian to the linear shape below 400 mK. This suggests that as the phase-coherence length L_ϕ grows longer trajectories which enclose a larger area begin to contribute to coherent backscattering at lower magnetic fields. (2) We present evidence that stable periodic orbits can exist in a ballistic cavity by observing a single periodicity Aharonov-Bohm effect at the lowest temperatures in certain nominally rectangular structures.

Whereas in the case of classical chaos the transition from nonchaotic to chaotic behavior has been studied extensively [9], intense experimental investigation of “quantum chaos” in open systems has only begun in recent years. Previous experimental studies of quantum chaos in microstructures have focused on the universal conductance fluctuations (UCF) and WL peak of individual cavities [10–12] or on the magnetoresistance of antidot arrays [13]. Marcus *et al.* [10] investigated the power spectrum of $G(B)$ for a stadium versus a circle; the fact that their circles showed more power at the higher frequencies than their stadia was the first experimental evidence for a difference between chaotic and nonchaotic behavior in quantum transport (exponential decay versus power law). The deviation occurred only after the power had decayed substantially, however, so that effects of elastic and inelastic scattering have to be carefully considered. In fact, the power spectrum for the circle can be fit by an exponential over one and a half decades; the resulting rate is smaller than for the stadium but is consistent with a reasonable estimate of the small-angle mean free path [8]. The possibility of differing interpretations of this work makes a clear observation of the difference between chaotic and nonchaotic cavities essential. Later studies concentrated on the magnetotransport of an individual stadium cavity [11,12] and therefore did not

address the issue of chaotic versus nonchaotic behavior. Finally, several studies [10,11,13], particularly that on the magnetoresistance of antidot arrays [13], have seen evidence for interference effects between short nonuniversal paths, such as the circular trajectories enclosing an antidot in the case of Ref. [13]. We return to this issue at the end of the paper.

Our devices are fabricated on a doping well GaAs/Al_xGa_{1-x}As heterostructure crystal with an electron density of $3.3 \times 10^{11} \text{ cm}^{-2}$ and a mobility of $1.8 \times 10^6 \text{ cm}^2/\text{Vs}$. Measurement is performed with a lock-in amplifier at 23 Hz at a current of 20 nA for $T \leq 1.6 \text{ K}$ and 100 nA at $T \geq 2.4 \text{ K}$. *Length scales:* The transport mean free path is $17 \mu\text{m}$ compared to a typical cavity diameter of $\leq 1.25 \mu\text{m}$. The small-angle scattering length is estimated from the observed 2% modulation of $G(B)$ (at $T = 0.5 \text{ K}$) due to electron focusing [14] for injection and collection point contacts separated by $11.6 \mu\text{m}$ in linear distance. Assuming an exponential decay in the number of unperturbed electrons as a function of distance, we deduce a small-angle scattering length of $4 \mu\text{m}$. The phase-coherence length L_ϕ is estimated to exceed $15 \mu\text{m}$ below 400 mK [15]. *Size:* The cavities are fabricated by electron beam lithography and ECR (low voltage reactive ion) etching. Both the stadium and circle cavities are fabricated in one electron beam write on the same device chip. The perimeter is defined via a 1500 \AA wide line etched to depletion. The lithographic dimension of the stadium, as shown in the inset of Fig. 1(a), is $1.25 \times 0.85 \mu\text{m}$ with a $0.4 \mu\text{m}$ straight portion. The circle of equivalent area is of diameter $1.08 \mu\text{m}$ [Fig. 1(b)]. The electron gas resides 568 \AA below the surface, and the etching is 200 \AA in depth. From the pinch-off characteristic of narrow constrictions $\approx 1000 \text{ \AA}$ wide, we estimate a depletion length of $300 \pm 100 \text{ \AA}$, yielding an area of $0.81 \mu\text{m}^2$ with a corresponding magnetic field scale of 51.4 G for one flux quantum penetrating the enclosed area. *Geometry:* The ratio of the entrance plus exit widths to the perimeter is roughly 1 to 6.5. Therefore, the number of phase coherent bounces before exiting is cut off mostly by the openings rather than L_ϕ when $T \leq 400 \text{ mK}$. The device for a given cavity type consists of 48 cavities arranged in 6 rows in a series of 8 in parallel. The spacing between rows is $25 \mu\text{m}$, comfortably larger than L_ϕ .

In Fig. 1 we show the weak-localization, negative magnetoresistance peak for the stadium and circle samples at 50 mK. The resistance value refers to that of a single cavity. The stadium WL peak can readily be fitted by a Lorentzian line shape with a peak height ΔG of $0.4e^2/h$ and a $B_{1/2}$ of $13 \pm 1 \text{ G}$. In contrast, the line shape for the circle is certainly non-Lorentzian, following an unusual linear decrease with magnetic field. The peak is characterized by $\Delta G = 0.22e^2/h$ and $B_{1/2} = 11 \pm 1 \text{ G}$. While we concentrate on studying the line shape, we note that the magnitude of the WL peak in the stadium is consistent with recent theoretical work [16]

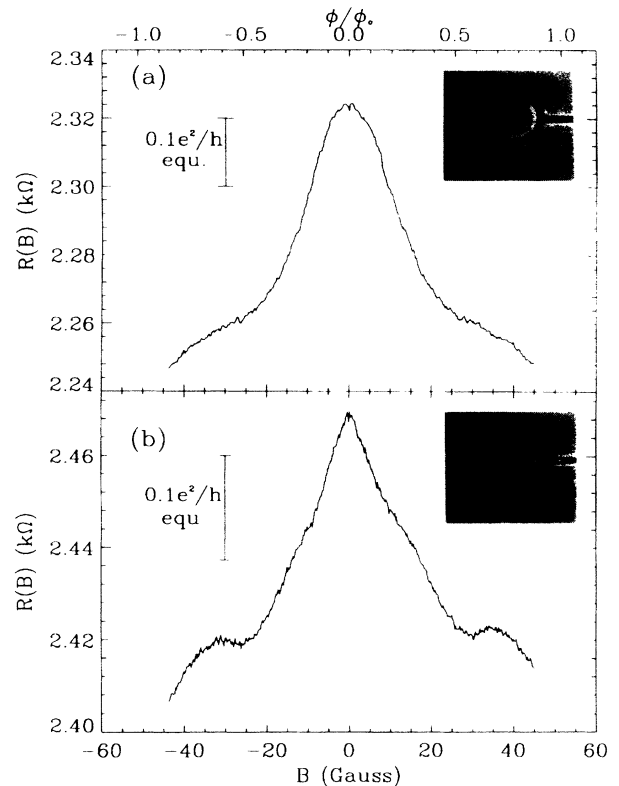


FIG. 1. The magnetoresistance for (a) 48 stadium cavities and (b) 48 circle cavities, normalized to a single cavity, at $T = 50 \text{ mK}$. The weak localization peak line shape shows a Lorentzian behavior for the chaotic, stadium cavities. In contrast, the line shape for the nonchaotic, circle cavities shows a highly unusual, triangular shape (linearly decreasing). The vertical bar indicates the equivalent change in conductance, ΔG . Insets show electron micrographs of the cavities which are fabricated on a high quality GaAs/Al_xGa_{1-x}As heterostructure crystal.

which predicts a universal magnitude of $0.25e^2/h$ per spin channel in the fully chaotic case.

The possibility of such an unusual line shape in a nonchaotic (integrable) system was first pointed out in the work of Baranger *et al.* [7] who gave a general semiclassical argument connecting the linear line shape to the existence of a power-law distribution of classical areas in a nonchaotic system. In order to demonstrate the connection between our experimental results and the theory, in Fig. 2 we show the change in conductance $[-\Delta G = G(B=0) - G(B)]$ obtained from numerical calculations for ballistic billiards which have the same nominal shape as the experimental structures. The conductance is calculated through its relation to the total transmission, $G = (e^2/h)T$, by using the recursive Green function method to obtain T for a discretized billiard (using $ka \approx 1.4$) [17]. The average conductance needed to make contact with the experiments is found by averaging over energy in the range for which there are 2–9 propagating modes in the leads.

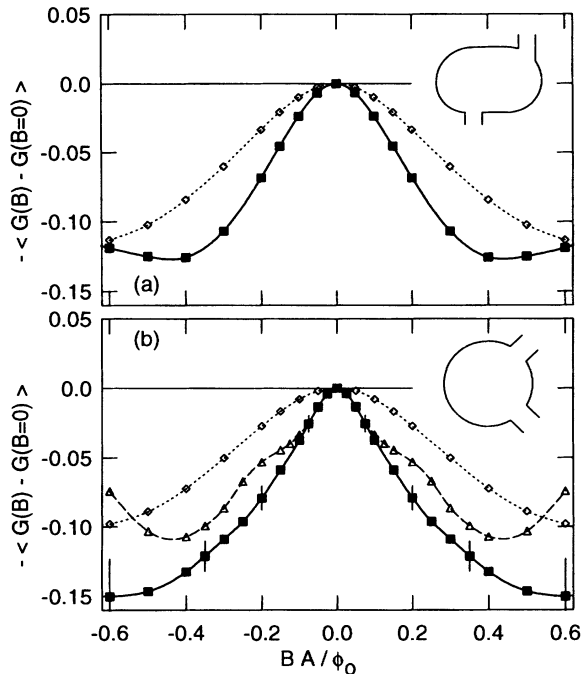


FIG. 2. Calculated magnetoconductance ($\times - 1$) as a function of flux through the geometric area of the cavity for the (a) stadium and (b) circle shown as insets. The line shape is Lorentzian for the ballistic stadium (solid squares) as well as for a stadium with strong surface roughness scattering (diamonds). The line shape is more triangular for both the ballistic circle (triangles) and the circle with a weak smooth disordered potential (solid squares), but changes to Lorentzian for strong surface roughness scattering (diamonds). For the disordered potential, the total mean free path is approximately five times the diameter of the cavity. The similarity of line shape between this calculation and the experiment (Fig. 1) is striking for both structures.

Note the clearly Lorentzian line shape for the stadium and the more triangular shape for the circle. The resemblance between experiment and theory is remarkable for both cavities. *We believe these results in combination provide strong evidence that chaotic and nonchaotic scattering in ballistic cavities indeed give rise to the experimentally observed difference in transport.*

An important issue in interpreting the experimental results is the influence of small-angle scattering. The first quantitative theoretical treatment was given by Lin, Delos, and Jensen [8]; they emphasize that small-angle scattering in a circle changes the classical distribution of areas from a power law to an exponential, but one whose characteristic area is different from that of a stadium with the same geometric area. Thus one must seriously consider the effects of any disorder even when the transport mean free path is large. We have carried out quantum calculations for the stadium and circle billiards in the presence of a smooth disordered potential. The disorder is formed by choosing a random value for the potential at every fifth lattice site (within a range $[-W_{\text{dis}}/2, W_{\text{dis}}/2]$) and linearly interpolating in between

[18]. The transport mean free path is 10–20 times larger than the total mean free path. Figure 2(b) shows that the linear WL line shape in the nonchaotic case is not destroyed by a smooth disordered potential whose strength is chosen so as to match the total and transport mean free paths in the experimental structures ($W_{\text{dis}} = 0.25$). For comparison we show that strong boundary roughness scattering does change the theoretical line shape to a Lorentzian, as expected ($W_{\text{dis}} = 5$ was used on the last meshpoint before the hard wall). We conclude that small-angle scattering is weak enough in these experiments so that the nonchaotic nature of the classical paths in the ideal circular cavity is actually observed.

Conclusive evidence that phase coherence is essential for the experimental observations is provided by the temperature evolution of the WL peak shown in Fig. 3. For the stadium, the line shape is Lorentzian for the entire temperature range, as shown for the Lorentzian fits at 50 mK and 1.6 K. On the other hand, while the circle appears to be Lorentzian-like at the higher temperatures, albeit with a slightly cusped peak at $B = 0$, the full linear

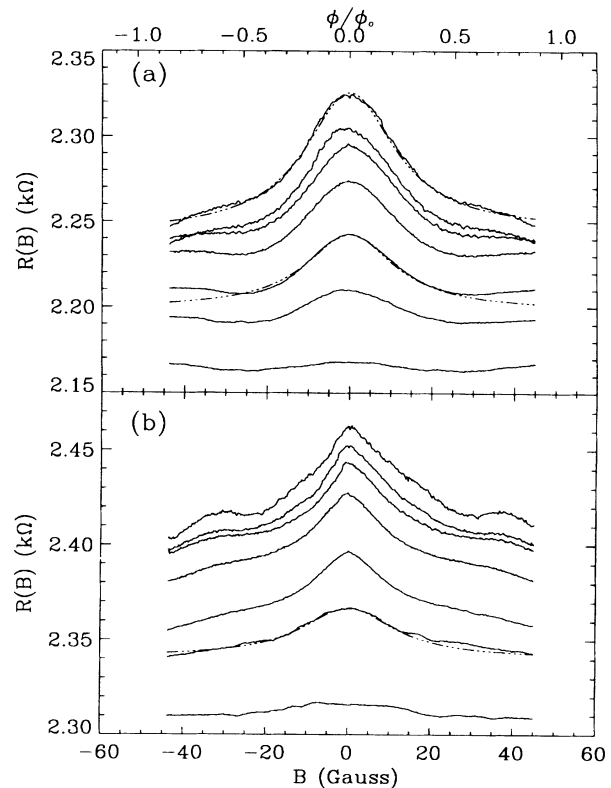


FIG. 3. The temperature evolution of the magnetoresistance for the (a) stadium cavities, and (b) circle cavities. From top to bottom, $T = 50$ mK, 200 mK, 400 mK, 800 mK, 1.6 K, 2.4 K, and 4.2 K. The dash-dotted lines are Lorentzian fits. For the stadium cavities, the weak localization line shape is Lorentzian at all temperatures. For the circle cavities, the line shape is Lorentzian only at higher temperatures above 2.4 K. The linearly decreasing triangular line shape develops fully below 400 mK, showing that phase coherence is essential in producing this shape.

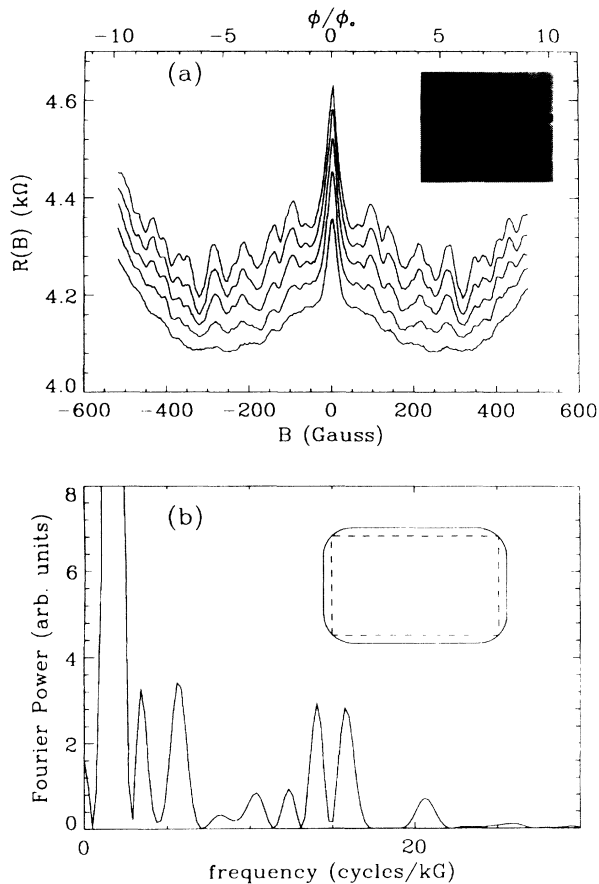


FIG. 4. (a) Magnetoresistance for 48 nominally rectangular cavities normalized to a single cavity. The traces correspond to the temperatures of 50 mK (top), 200 mK, 400 mK, 800 mK, and 1.6 K (bottom), with each successive trace displaced downward by 0.6 k Ω . In addition to the weak-localization peak at $B = 0$, periodic modulation of the magnetoresistance is present, probably caused by interference around a periodic orbit in the structure. Panel (b) shows that the Fourier power spectrum exhibits double peaks at 14 and 16 cycles/kG. The inset to panel (a) contains an electron micrograph of the cavity. The inset to panel (b) delineates a possible periodic orbit (dashed lines) inside the cavity (solid curve) for which lateral depletion of the 2D electron gas from etching has rounded the corners.

behavior develops below ≈ 400 mK. It appears that the longer trajectories which enclose larger areas and contribute to the negative magnetoresistance at the smaller B fields become sufficiently phase coherent only at these lower temperatures.

While the general WL lineshape discussed above is related to the full distribution of areas of classical paths, semiclassical theory also suggests that interference between short nonuniversal paths should produce magnetotransport effects particular to certain shapes. Indeed, some experimental evidence for the role of small area trajectories has already been reported [10,11,13]. In Fig. 4, we present particularly clear evidence for the existence of a stable periodic orbit in a nominally rectangular cavity of $1.2 \times 0.75 \mu\text{m}$; the magnetoresistance shows

pronounced modulation as a function of B at low temperatures ≤ 400 mK. The Fourier power spectrum exhibits double peaks at 14 and 16 cycles/kG. The average period of 67 G corresponds to an area of $0.62 \mu\text{m}^2$ for the penetration of one flux quantum compared to an estimated area of $0.79 \mu\text{m}^2$ for the cavity. The inset shows a possible periodic orbit. Because this result is obtained in a device containing 48 cavities, we believe this is strong evidence for the existence of a stable orbit common to a significant fraction of all cavities.

We thank D.J. Bishop for support and continued interest in the course of this work.

- [1] For reviews of quantum-chaotic scattering, see M.C. Gutzwiller, *Chaos in Classical and Quantum Mechanics* (Springer-Verlag, New York, 1991); and U. Smilansky, in *Chaos and Quantum Physics*, edited by M.-J. Giannoni, A. Voros, and J. Zinn-Justin (North-Holland, New York, 1991).
- [2] R. Blümel and U. Smilansky, Phys. Rev. Lett. **60**, 477 (1988); Physica (Amsterdam) **36D**, 111 (1989); E. Doron, U. Smilansky, and A. Frenkel, Physica (Amsterdam) **50D**, 367 (1991).
- [3] R.A. Jalabert, H.U. Baranger, and A.D. Stone, Phys. Rev. Lett. **65**, 2442 (1990).
- [4] C.H. Lewenkopf and H.A. Weidenmüller, Ann. Phys. (N.Y.) **212**, 53 (1991).
- [5] R.B.S. Oakeshott and A. MacKinnon, Superlattices Microstruct. **11**, 145 (1992).
- [6] Y.-C. Lai, R. Blümel, E. Ott, and C. Grebogi, Phys. Rev. Lett. **68**, 3491 (1992).
- [7] H.U. Baranger, R.A. Jalabert, and A.D. Stone, Phys. Rev. Lett. **70**, 3876 (1993); Chaos **3**, 665 (1993).
- [8] W.A. Lin, J.B. Delos, and R.V. Jensen, Chaos **3**, 655 (1993).
- [9] See, for example, E. Ott, *Chaos in Dynamical Systems* (Cambridge University Press, New York, 1993); and A. Davidson, B. Dueholm, and M.R. Beasley, Phys. Rev. B **33**, 5127 (1986).
- [10] C.M. Marcus, A.J. Rimberg, R.M. Westervelt, P.F. Hopkins, and A.C. Gossard, Phys. Rev. Lett. **69**, 506 (1992); C.M. Marcus, R.M. Westervelt, P.F. Hopkins, and A.C. Gossard, Phys. Rev. B **48**, 2460 (1993); Chaos **3**, 643 (1993); Surf. Sci. **305**, 480 (1994).
- [11] M.W. Keller, O. Millo, A. Mittal, D.E. Prober, and R.N. Sacks, Surf. Sci. **305**, 501 (1994).
- [12] M.J. Berry, J.H. Baskey, R.M. Westervelt, and A.C. Gossard (to be published); Surf. Sci. **305**, 495 (1994).
- [13] D. Weiss, K. Richter, A. Menschig, R. Bergmann, H. Schweizer, K. von Klitzing, and G. Weimann, Phys. Rev. Lett. **70**, 4118 (1993).
- [14] H. van Houten *et al.*, Europhys. Lett. **5**, 721 (1988).
- [15] C. Kurdak, A.M. Chang, A. Chin, and T.Y. Chang, Phys. Rev. B **46**, 6846 (1992), and references therein.
- [16] H.U. Baranger and P.A. Mello, Phys. Rev. Lett. **73**, 142 (1994); R.A. Jalabert, J.-L. Pichard, and C.W.J. Beenakker, Europhys. Lett. **27**, 255 (1994).
- [17] H.U. Baranger *et al.*, Phys. Rev. B **44**, 10637 (1991), and references therein.
- [18] H.U. Baranger, Phys. Rev. B **42**, 11479 (1990).

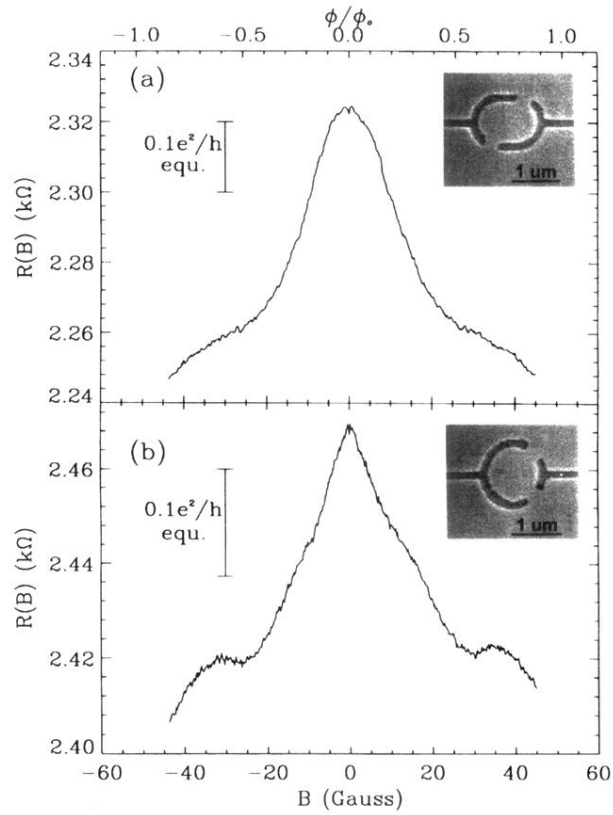


FIG. 1. The magnetoresistance for (a) 48 stadium cavities and (b) 48 circle cavities, normalized to a single cavity, at $T = 50$ mK. The weak localization peak line shape shows a Lorentzian behavior for the chaotic, stadium cavities. In contrast, the line shape for the nonchaotic, circle cavities shows a highly unusual, triangular shape (linearly decreasing). The vertical bar indicates the equivalent change in conductance, ΔG . Insets show electron micrographs of the cavities which are fabricated on a high quality GaAs/ Al_xGa_{1-x} As heterostructure crystal.

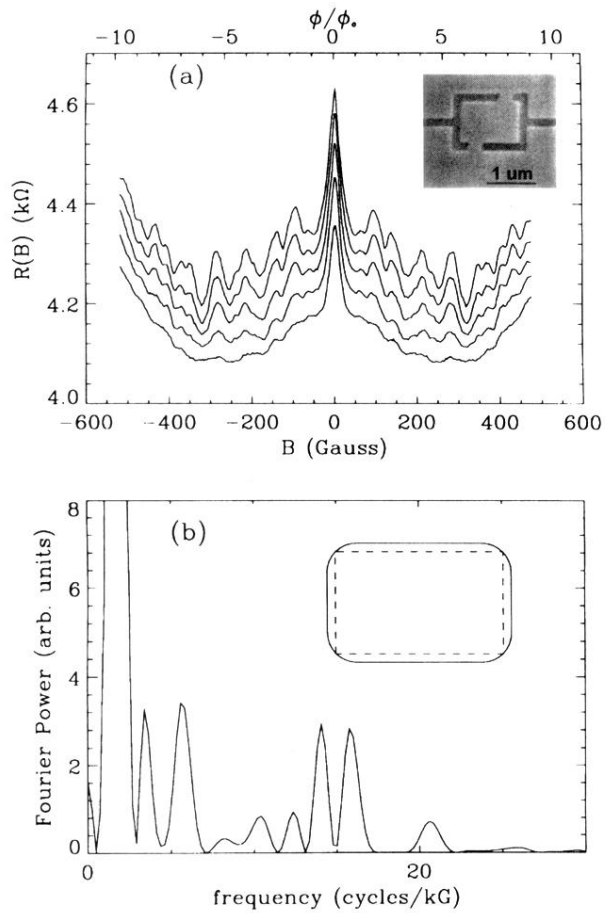


FIG. 4. (a) Magnetoresistance for 48 nominally rectangular cavities normalized to a single cavity. The traces correspond to the temperatures of 50 mK (top), 200 mK, 400 mK, 800 mK, and 1.6 K (bottom), with each successive trace displaced downward by 0.6 k Ω . In addition to the weak-localization peak at $B = 0$, periodic modulation of the magnetoresistance is present, probably caused by interference around a periodic orbit in the structure. Panel (b) shows that the Fourier power spectrum exhibits double peaks at 14 and 16 cycles/kG. The inset to panel (a) contains an electron micrograph of the cavity. The inset to panel (b) delineates a possible periodic orbit (dashed lines) inside the cavity (solid curve) for which lateral depletion of the 2D electron gas from etching has rounded the corners.